

Non-isothermal crystallization kinetics and thermal stability of the in situ reinforcing composite films based on thermotropic liquid crystalline polymer and polypropylene

Sayant Saengsuwan · Pongsathorn Tongkasee ·
Taweesak Sudyoadsuk · Vinich Promarak ·
Tinnagon Keawin · Siriporn Jungstittiwong

Received: 1 June 2010 / Accepted: 24 August 2010 / Published online: 10 September 2010
© Akadémiai Kiadó, Budapest, Hungary 2010

Abstract The non-isothermal crystallization kinetics and thermal stability of the in situ reinforcing composite thin film, comprising of 10 wt% of thermotropic liquid crystalline polymer (TLCP, Rodrun LC5000) and polypropylene (PP), prepared by a two-step method were investigated using differential scanning calorimetry (DSC) and thermogravimetry (TG), respectively. The DSC results revealed that Mo method was suitable for the crystallization behavior description of both neat PP and 10 wt% TLCP/PP films. The in situ formation of TLCP fibrils in the PP matrix led to reduction in both values of half-time of crystallization ($t_{1/2}$) and the kinetic parameter of Mo equation $F(T)$, resulting in a significant increase in the crystallization rate of PP phase. The remarkable lower in crystallization activation energy of the composite films also confirmed that in situ formed TLCP fibrils could influence the molecular chain of PP easier to crystallize, and hence resulted in the faster crystallization rate. The nucleation activity value of composite indicated that TLCP fibrils acted as effective nucleating agents. From TG results and the higher decomposition activation energy, the thermal stability of the composite can be improved by the presence of in situ-formed TLCP fibrils.

Keywords Liquid crystalline polymer · PP · Composites · Crystallization · Kinetics · Thermal stability

Abbreviations

DSC	Differential scanning calorimetry
DTG	Differential thermogravimetry
HBA	<i>p</i> -Hydroxy benzoic acid
PBT	Poly(butylene terephthalate)
PET	Polyethylene terephthalate
PP	Polypropylene
TG	Thermogravimetric analyzer
TLCP	Thermotropic liquid crystalline polymer
TP	Thermoplastic
ΔE	Activation energy
k	The rate constant of Avrami equation
k_c	The kinetic crystallization rate constant
$K(T)$	The kinetic parameter of Ozawa equation
$F(T)$	The kinetic parameter of Mo equation
m	Ozawa exponent
n	Avrami exponent
t	Time
$t_{1/2}$	Half-time of crystallization
T_c	Crystallization temperature
T_o	The onset crystallization temperatures
T_∞	The end crystallization temperature
T_{max}	The maximum decomposition temperature
T_{onset}	The onset decomposition temperature
X_t	Relative crystallinity
ϕ	Cooling rate
θ	Nucleation activity
θ	$T - T_{max}$

S. Saengsuwan (✉) · P. Tongkasee · T. Sudyoadsuk ·
V. Promarak · T. Keawin · S. Jungstittiwong
Center for Organic Electronics and Polymers, Department
of Chemistry and Center for Innovation in Chemistry,
Faculty of Science, Ubon Ratchathani University,
Warinchamrap, Ubon Ratchathani 34190, Thailand
e-mail: scsayasa@ubu.ac.th

Introduction

Since the last two decades, thermotropic liquid crystalline polymers (TLCPs) have gained much research attention in both academic and industrial fields, due to its various

advantages such as superior strength/modulus, low melt viscosity, low gas permeability, and high chemical/thermal resistances [1–3]. Therefore, TLCPs have been used to blend with a variety of thermoplastics (TPs) to obtain the composite-like materials with a strongly mechanical reinforcement of the polymer matrix [1–6]. However, most TLCP/TPs blends exhibited a two-phase morphology. As in the molten state, the dispersed TLCP droplets can be elongated under a sufficient shear or extensional forces and after rapid solidification, a TLCP fibrillar morphology is formed producing a so-called in situ composite [7] with significantly enhanced mechanical properties in the fiber orientation direction. Moreover, addition of TLCP to a TP also resulted in a remarkable reduction of the melt viscosity of the blend, and thus acted as a processing aid with subsequent reduction of wear in processing equipments [4, 6, 8]. Nevertheless, the mechanical properties of the resulting in situ composites are controlled by their morphology, which in turn depends on the rheological properties of the blend, blend composition, interfacial adhesion, and processing conditions [9–11]. Thus, by controlling the morphology, the mechanical performance of in situ polymer composites can be improved. Various fabrication techniques, i.e., fiber spinning, injection molding, and sheet extrusion, have been used so far to generate the in situ composites, sheets and films of composites are typically done by sheet extrusion. The advantages of film fabrication over other techniques as there are no skin–core effects and no weld-line formation in the sample. To avoid such effects, we thus prepared the TLCP/PP in situ composite film by the sheet extrusion technique.

Polypropylene (PP) is one of the largest used polyolefin in plastics industry due to its several excellent properties coupled with ease processing and low price. Also, PP is used in several applications, i.e., packaging, fibers, film, pipes, transportation, and electrical/electronic applications, etc. The application ranges of PP can be expanded by addition of nanoparticles/clays into PP matrix to fabricate the nanocomposite materials [12–14]. In addition, PP can be modified by blending with TPs [15–17] and TLCPs [5–7, 10, 11]. Despite the fact that various kinds of TLCPs, such as Vectra A, Vectra B, and Rodrun LC3000 have been used to blend with PP, only few works reported on the composite system comprising of PP and Rodrun LC5000. Bualek-Limchroen et al. [6, 18] have studied the properties of Rodrun LC5000/PP in situ composite in the forms of as-spun/drawn monofilaments and extrusion thin film. They concluded that the incorporation of Rodrun LC5000 into PP remarkably improve processability and significantly enhance both modulus and tensile properties in machine direction of the in situ composites. However, they did not report on the crystallization kinetics and thermal stability of this composite system.

It is well known that the mechanical properties of the resulting TLCP/TPs in situ composite systems are strongly dependent on morphology developed, blend composition and the extent of crystallization, which in turn depends on the rheological properties, processing conditions and crystallization behavior of the blend system [1–3, 8–10]. In order to determine the effect of the complex thermal conditions during processing and to achieve the desired morphology and properties of the composites, it is important to study the crystallization kinetics during non-isothermal conditions and its relationship to the final properties. Practically, this is because the most industrial processing techniques generally proceed under dynamic non-isothermal conditions. Although, several authors have studied the crystallization kinetics of TLCP/TP blends [19–26], there are some conflicting results in the effect of TLCPs on the crystallinity of crystalline polymers. In some reports, TLCPs acted as nucleating agents for the spherulites during crystallization process of poly(phenylene sulfide), poly(butylene terephthalate) (PBT) and poly(ethylene 2,6-naphthalate) [19–22]. However, other works suggested that the crystallization rate of poly(aryl ether ether ketone) and PBT tended to be decreased [23, 24]. Moreover, few works have studied on crystallization kinetics of the TLCP/PP blends. Torre et al. [25], for instance, studied the isothermal crystallization of PP/Vectra A950 blend and concluded that Vectra domains acted as sites for the nucleation of PP, and the crystallization rate was enhanced with Vectra contents. While Tjong et al. [26] reported that TLCP phase does not act as nucleating sites for PP spherulites under isothermal crystallization, but TLCP domain leads to slightly increase in the crystallization rate of Vectra A950 blended with PP and maleic anhydride grafted PP.

Many kinetic models such as Avrami, Ozawa, and Mo methods have been used to describe the crystallization behavior of the PP phase and its blend systems. However, in each a particular system, the suitable models for describing the crystallization behaviors is varied [12–14, 25, 26]. Also, there is little information on the crystallization kinetics and thermal stability of PP in situ reinforced by TLCPs microfibrils, especially in the system of Rodrun LC5000/PP fabricated as an extruded thin film, according to author's knowledge. Thus, in this work, we are interested to investigate the non-isothermal crystallization kinetics and thermal stability of an extruded thin film of PP in situ reinforced by TLCP (Rodrun LC5000) using differential scanning calorimetry (DSC) and thermogravimetry (TG), respectively. The models of modified Avrami, Ozawa, and Mo were employed to achieve the relevant kinetic parameters. The crystallization activation energies based on Kissinger's method and nucleation activity were also calculated. Finally,

the thermal stability and decomposition activation energy of TLCP/PP in situ composites were also investigated.

Experimental

Materials

PP, PRO-FAX 6631, with a melt flow index of 2 g per 10 min, kindly provided by HMC Co., Thailand, was used as a matrix phase. The in situ reinforcing phase was TLCP (Rodrun LC5000), a copolyester of 80% mol *p*-hydroxy benzoic acid (HBA)/20% mol polyethylene terephthalate (PET), purchased from Unitika Co., Japan. The melting temperature and a density of TLCP are 280 °C and 1.41 g cm⁻³, respectively. All materials were dried in a vacuum oven at 80 °C for 10 h before use.

Blending and fabrication of in situ composite films

The composite films were prepared by using a two-step method. A detailed description of the process was presented elsewhere [6]. Briefly, PP pellets were first melt-blended with 10 wt% of TLCP in a twin-screw extruder and then were fabricated as a cast thin film through a mini-extruder. The film with a high draw ratio of 30 (a die gap to film thickness), corresponding to the film thickness of about 22 μm, was prepared and used throughout this work.

Non-isothermal crystallization kinetics

The non-isothermal crystallization of 10 wt%TLCP/PP and neat PP films was studied by DSC, Mettler Toledo, 823°. All DSC measurements were carried out in nitrogen atmosphere. Samples cut into small pieces of about 3–4 mg were used. The samples were initially melted at 200 °C for 5 min to remove their thermal history. Then the samples were cooled from 200 to 30 °C at four different cooling rates of 5, 10, 15, and 20 °C min⁻¹, respectively. The experimental data were then recorded and analyzed using a package software program “Star[®] 9.0”.

Thermal stability

The thermal stability of the 10 wt%TLCP/PP and neat PP films were performed by a thermogravimetric analyzer (TG), Rigaku TG8120. Film samples cut into small pieces of about 3–4 mg were heated at a scanning rate of 10 °C min⁻¹ from 30 to 800 °C under nitrogen atmospheres. The onset decomposition temperatures (T_{onset}), the maximum thermal decomposition temperatures (T_{max}) were reported. Finally, the decomposition activation energy (ΔE) of samples were evaluated.

Results and discussion

Non-isothermal crystallization behavior

Crystallization exotherms at different cooling rates of neat PP and 10 wt%TLCP/PP films are presented in Fig. 1. As expected, crystallization temperature (T_c) shifts to lower temperature with increasing cooling rate for both samples, due to a larger supercooling at higher cooling rates (see Table 1). For each cooling rate, T_c and crystallization exotherm broadness of the composite films are higher and narrower, respectively, than those of neat PP film. These results imply that the crystallization process of composite film is shorter than that of neat PP film, and it also suggests that the in situ formed TLCP fibrils act as nucleating sites for PP crystallization.

Relative crystallinity (X_t) as a function of crystallization temperature (T) and time (t) can be acquired from the crystallization exotherms of samples as follows:

$$X_t = \frac{\int_{T_0}^T (dH/dT)dT}{\int_{T_0}^{T_\infty} (dH/dT)dT} \quad (1)$$

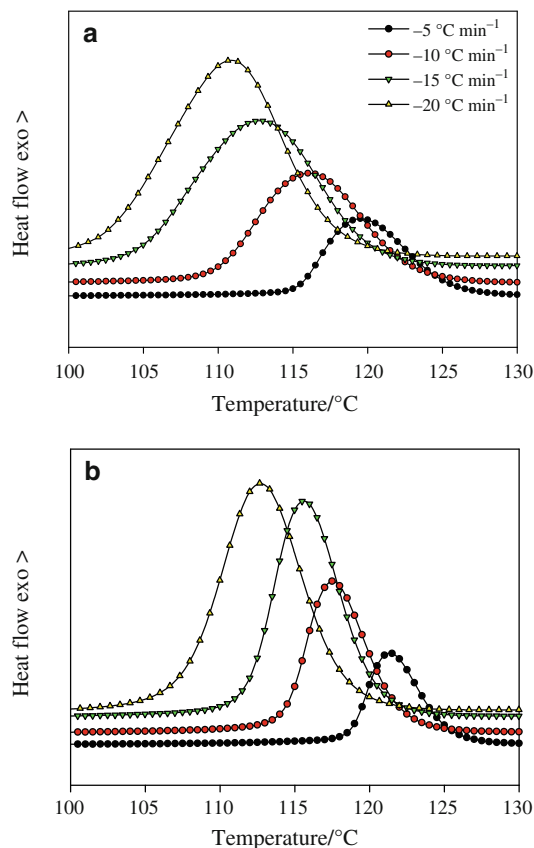


Fig. 1 DSC thermograms of **a** neat PP and **b** 10 wt%TLCP/PP films during non-isothermal crystallization at different cooling rates

Table 1 Non-isothermal crystallization kinetic parameters for PP and 10 wt%TLCP/PP films

Samples	$\phi/^\circ\text{C min}^{-1}$	$T_c/^\circ\text{C}$	$t_{1/2}/\text{min}$	$1/t_{1/2}/\text{min}^{-1}$	n	k	k_c	R^2
Neat PP	5	119.5	2.81	0.356	5.1	0.003	0.313	0.9910
	10	116.7	1.43	0.669	4.4	0.138	0.820	0.9955
	15	112.5	1.06	0.990	4.5	0.625	0.969	0.9987
	20	110.5	0.82	1.219	5.0	1.553	1.022	0.9982
10 wt%TLCP/PP	5	121.4	1.71	0.585	4.8	0.052	0.554	0.9975
	10	117.4	1.15	0.869	5.7	0.287	0.883	0.9966
	15	115.6	0.98	1.020	5.8	2.132	1.052	0.9975
	20	112.5	0.72	1.389	5.8	4.007	1.072	0.9983

where T_o and T_∞ represent the onset and end crystallization temperatures, respectively. During non-isothermal crystallization process, the relationship between crystallization time (t) and temperature (T) is given as follows:

$$t = (T_o - T)/\phi \quad (2)$$

where t is the crystallization time and ϕ is cooling rate. The plots of X_t versus t , for both samples at various cooling rates are shown in Fig. 2. It is seen that all curves show a similar sigmoidal shape and the upper part of all curves in the plot is also found to be level off due to the spherulites

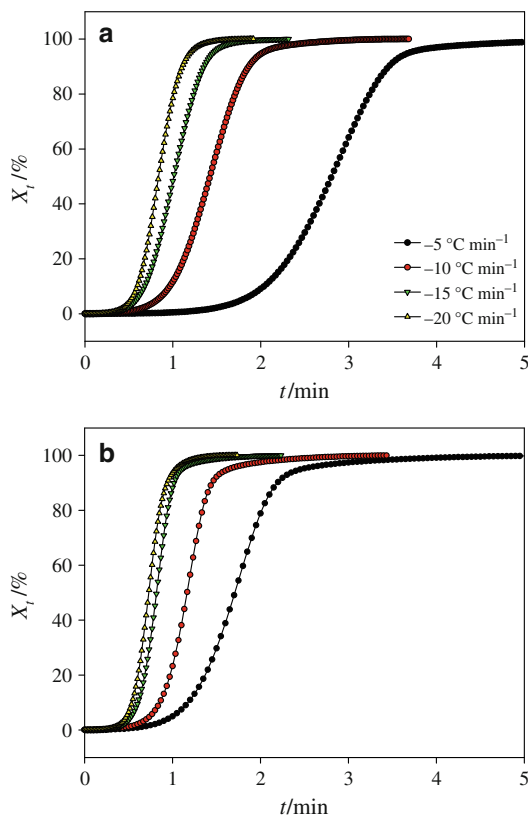


Fig. 2 Relative crystallinity versus time for non-isothermal crystallization of **a** neat PP and **b** 10 wt%TLCP/PP films at different cooling rates

impingement. With increasing cooling rates, the sigmoidal shapes are shifted to lower temperature of shorter time for completing the crystallization. From Fig 2, half-time of crystallization, $t_{1/2}$, can be obtained when the X_t are equal to 50%, and the parameters are listed in Table 1. The value of $t_{1/2}$ directly indicate the crystallization rate and the reciprocal of $t_{1/2}$ value (time^{-1}) is usually used to compare the crystallization rates of different systems, i.e., long $t_{1/2}$ or less $1/t_{1/2}$ indicates the slow crystallization [27]. As seen in Table 1, $t_{1/2}$ values of both samples decrease with increasing cooling rates, indicating a progressively faster crystallization rates as the cooling rate increases. Furthermore, $1/t_{1/2}$ values of 10 wt%TLCP/PP films are higher than those of the neat PP film at each cooling rates, indicating the higher overall crystallization rate of 10 wt%TLCP/PP film than neat PP one. Therefore, according to $t_{1/2}$ and $1/t_{1/2}$ values, it could be concluded that the TLCP fibrils act as a nucleating agent and accelerate the overall crystallization process of PP phase.

Non-isothermal crystallization kinetic analysis

Analysis based on the Avrami theory modified by Jeziorny

Avrami theory [28] is generally used for analyzing the primary stage of isothermal crystallization kinetics. This approach ignores the effect of cooling rate and thermal gradients within the sample. According to the model, the relative crystallinity (X_t) develops with crystallization time (t) as follows:

$$X_t = 1 - \exp(-kt^n) \quad (3)$$

$$\ln[-\ln(1 - X_t)] = \ln k + n \ln t \quad (4)$$

where n is Avrami exponent depending on crystal growth mechanism, and k is the rate constant involving both nucleation and growth rate parameters. Both n and k can be obtained from the slope and intercept of the curves, respectively. In order to make this model applicable to the non-isothermal crystallization process, Jeziorny [29] thus

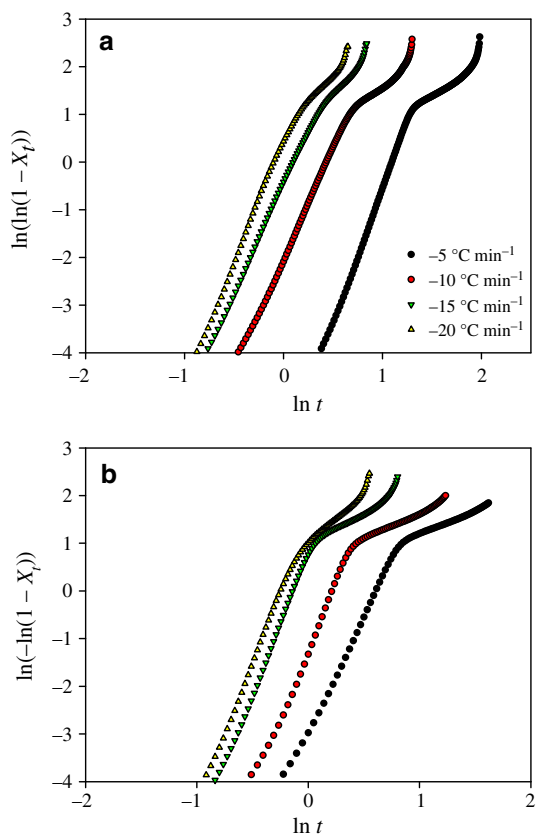


Fig. 3 Avrami plots of $\ln(-\ln(1 - X_t))$ versus $\ln t$ for non-isothermal crystallization of **a** neat PP and **b** 10 wt%TLCP/PP films

considered to correct the crystallization rate constant by introducing the cooling rate (ϕ) because temperature changed at a given cooling rate affects the rate of both nucleation and spherulite growth which are temperature dependent parameter. The modified equation is expressed as follows:

$$\ln k_c = \ln k / \phi \tag{5}$$

where k_c is the kinetic crystallization rate constant. Figure 3 presents Avrami plots of the neat PP and 10 wt%TLCP/PP films at various cooling rates. Each curve in Fig. 3 exhibits good linear relationship except a secondary crystallization at the latter crystallization state, normally considering to be due to the slow crystallization and further perfection of crystals. However, the modified Avrami equation can be used to describe a large range of relative crystallinity. Thus, the linear line in the middle portion of the curves in Fig. 3 is adopted to determine Avrami exponent (n) and the corresponding rate parameters as listed in Table 1. The average values of n for neat PP and 10 wt%TLCP/PP films are 4.8 and 5.5, respectively. The Avrami exponent $n > 4$ indicates a more complicated nucleation type and spherulite growth form. Also, the average exponent n for 10 wt%TLCP/PP was larger than that for neat PP film indicating that the

non-isothermal crystallization of the composite corresponds to solid sheaf-like growth with heterogeneous nucleation, and the TLCP fibrils acted as sites for nucleation in PP matrix [14, 30]. The values of k and k_c of both samples slightly increase with increasing cooling rates, since both parameters are the measurement of crystallization rate that gets faster with increasing cooling rate. Furthermore, at a given cooling rates, the k_c values of composite is higher than those of neat PP film, demonstrating that the crystallization rates of composite films are higher than neat PP one corresponding to the $t_{1/2}$ and $1/t_{1/2}$ values as discussed earlier.

Analysis based on the Ozawa method

The mostly used kinetic model for analyzing the non-isothermal crystallization process of polymers is Ozawa method [31]. This method extended the Avrami equation by assuming that the crystallization process is composed of small isothermal crystallization steps (i.e., replacing the time variable with cooling rate term) [32] and developed a formula as follows:

$$X_t = 1 - \exp(-K(T)/\phi^m) \tag{6}$$

$$\ln[-\ln(1 - X_t)] = \ln K(T) - m \ln \phi \tag{7}$$

where $K(T)$ is the function of cooling rate related to overall crystallization rate indicating how fast crystallization proceeds, which takes into account the geometry and change in nucleation density and growth rate, and m is the Ozawa exponent (similar to n but in different form) depending on the dimension of crystal growth. By plotting $\ln[-\ln(1 - X_t)]$ versus $\ln \phi$ at a given temperature, a series of straight line could be obtained if the Ozawa method was valid where the crystallization kinetic parameters $K(T)$ and m can be derived from the intercept and slope, respectively. The results of the Ozawa analysis for neat PP and composite films are presented in Fig. 4. It is clearly seen that most curves in the plots did not exhibit a linear relationship, especially at low temperature (114 °C). Moreover, there is a variation of slope as a function of temperature suggesting that m is not a constant during the process of non-isothermal crystallization. This observation can be explained as the crystallization processes at a given temperature with different cooling rates are at different stages, i.e., at higher cooling rate, the crystallization process is at an earlier stage and vice versa [12]. In addition, the Ozawa method ignored the secondary crystallization and the dependence of the lamellar thickness on crystallization temperature [32]. In general, a large portion of crystallinity is attributed to the secondary crystallization, especially for semi-crystalline polymers such as isotactic PP. From these information, it could be stated that m depends not only on

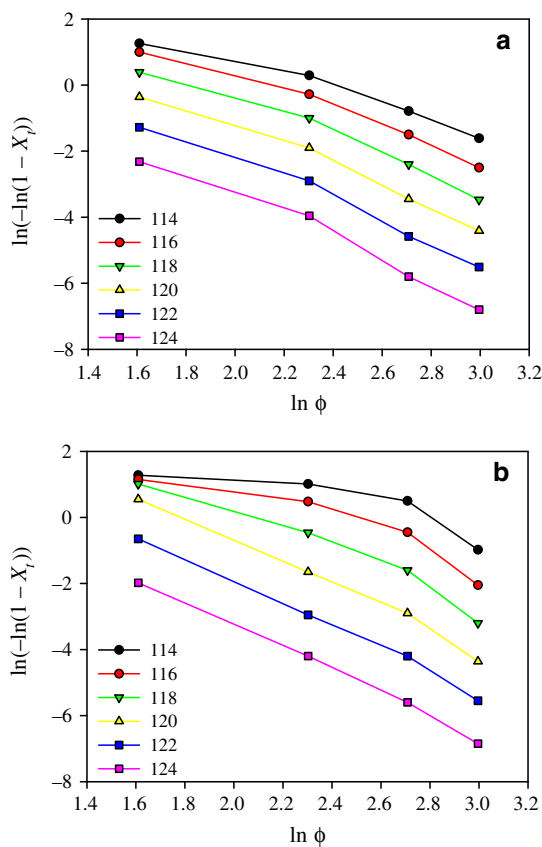


Fig. 4 Ozawa plots of $\ln(-\ln(1 - X_t))$ versus $\ln \phi$ for non-isothermal crystallization of **a** neat PP and **b** 10 wt%TLCP/PP films

the dimension of crystal growth, but also on other parameters such as time-dependent nucleation, variant growth rate constant as well as a combination of homogeneous and heterogeneous nucleation [21, 30, 32, 33]. As a consequence, the Ozawa analysis is not adequately applicable for studying the non-isothermal crystallization process of both neat PP and 10 wt%TLCP/PP films.

Analysis based on the Mo theory

In order to better describe the overall process of the non-isothermal crystallization process of neat PP and 10 wt% TLCP/PP films, Mo method has been applied. Liu et al. [34] proposed an alternative kinetic equation by combining the Avrami (Eq. 4) and Ozawa (Eq. 7) equations, which is given by:

$$\ln \phi = \ln F(T) - \alpha \ln t \quad (8)$$

where $F(T) = [K(T)/k]^{1/m}$ and $\alpha = n/m$, the ratio of the Avrami exponent n to the Ozawa exponent m . The kinetic parameter of Mo $F(T)$ refers to the value of cooling rate chosen at a unit crystallization time when system amounted to a certain degree of crystallinity, relating to the difficulty of the crystallization process for that particular material.

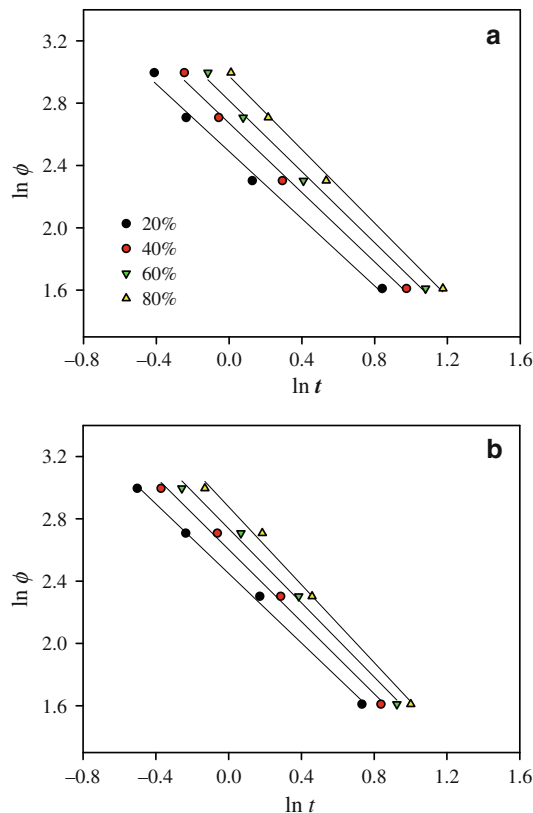


Fig. 5 Plots of $\ln \phi$ versus $\ln t$ from the Mo method for non-isothermal crystallization of **a** neat PP and **b** 10 wt%TLCP/PP films

The smaller value of $F(T)$, the higher crystallization rate or vice versa. And the importance of this method, the cooling rate was correlated to temperature and time of the non-isothermal crystallization process. Therefore, $F(T)$ has both definite physical and practical meaning. According to Eq. 8, at a given X_t , the plot of $\ln \phi$ versus $\ln t$ should yield a straight line with $\ln F(T)$ and α as the intercept and slope, respectively, if Mo analysis is valid. As seen in Fig. 5, plotting of $\ln \phi$ against $\ln t$ for neat PP and composite films shows a good linearity at a given X_t , verifying that the Mo method is applicable to the both systems. The values of α and $F(T)$ are evaluated and summarized in Table 2. It is seen that the value of α for neat PP and composite samples varies from 1.09 to 1.18 and 1.12 to 1.25, respectively. In addition, the values of $F(T)$ systematically increase with increasing the relative crystallinity, suggesting that at a unit crystallization time, a higher cooling rate is required to obtain a higher degree of crystallinity. The $F(T)$ values of neat PP sample are found to vary from 12.06 to 19.49, while those of composite sample are in the range of 11.59–17.63, as the X_t is increased. Moreover, the $F(T)$ values of composite sample at each given crystallinity are found to be smaller than those of neat PP, i.e., to reach the same X_t , the 10 wt%TLCP/PP sample needs smaller cooling rates because it crystallizes at a faster rate than the neat PP one.

Table 2 Crystallization kinetic parameters obtained from Mo method and crystallization activation energy of PP and 10 wt%TLCP/PP films calculated by Kissinger method

Samples	X_t	α	$F(T)$	R^2	$-\Delta E/\text{kJ mol}^{-1}$
Neat PP	20	1.08	12.06	0.9922	269
	40	1.11	14.44	0.9948	
	60	1.14	16.78	0.9950	
	80	1.18	19.49	0.9967	
10 wt%TLCP/PP	20	1.12	11.59	0.9975	210
	40	1.16	13.46	0.9963	
	60	1.19	15.49	0.9942	
	80	1.25	17.63	0.9943	

This result suggests that TLCP fibers act as a heterogeneously nucleating agent and accelerate the crystallization of PP.

Activation energy of crystallization by Kissinger method

In order to evaluate the effective energy barrier for non-isothermal crystallization process, the Kissinger method [35] has been employed. From this method, the activation energy (ΔE) for transporting of the macromolecular segments to the growing crystal surface can be determined. The equation is written as follows:

$$d[\ln(\phi/T_c^2)]/d(1/T_c) = -[\Delta E/R] \tag{9}$$

where T_c , ϕ , ΔE and R are the crystallization temperature, cooling rate, the crystallization activation energy and the gas constant, respectively. From the plot of $\ln(\phi/T_c^2)$ versus ($1/T_c$), as shown in Fig. 6, the crystallization activation energy (ΔE) can be calculated from the slope as listed in Table 2. The ΔE values of neat PP and composite films are

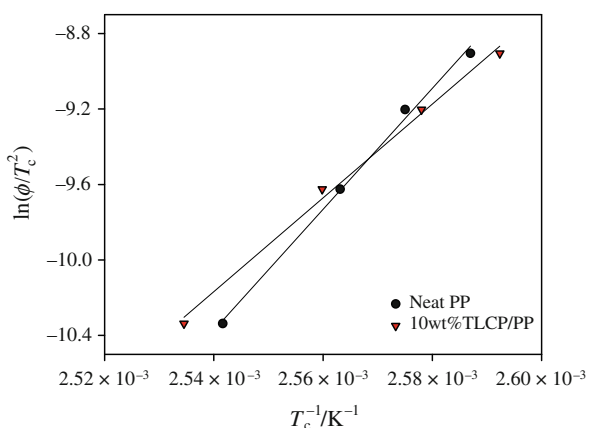


Fig. 6 Kissinger plots of $\ln(\phi/T_c^2)$ versus $1/T_c$ for calculating the non-isothermal crystallization activation energies of neat PP and 10 wt%TLCP/PP films

found to be 269 and 210 kJ mol^{-1} , respectively. The ΔE value of the composite sample strongly decreases compared to that of neat PP one. This implies that TLCP fibrils influence the PP chains to crystallize easier and accelerate the rate of crystallization during the non-isothermal crystallization process [14]. This result is also in good accordance with the higher crystallization rate of 10 wt%TLCP/PP, obtained from the modified Avrami and Mo method.

Nucleation activity

A simple approach for estimating the nucleation activity of foreign substrates in polymer melt was suggested by Dobreva et al. [36, 37]. Nucleation activity (ϕ) is a factor by which the work of three-dimensional nucleation decreases with the incorporating of a foreign agent. If the foreign agent is extremely active, ϕ approximates 0 and reaches 1 for inert agents. The ϕ is calculated from the ratio:

$$\phi = B^*/B \tag{10}$$

where B is a parameter calculating from the following relation:

$$B = \omega\sigma^3 V_m^2 / 3nkT_m \Delta S_m^2 \tag{11}$$

where ω is geometric factor, σ is the specific energy, V_m is the molar volume of the crystallizing substance, k is the Boltzmann constant, and ΔS_m is the entropy of melting. In addition, B can be experimentally examined from the slope of Eq. 12 obtained by plotting $\ln \phi$ and $1/\Delta T_c^2$:

$$\ln \phi = A - (B/\Delta T_c^2) \tag{12}$$

where A is a constant, and ΔT_c is the degree of supercooling, i.e., $\Delta T_c = T_m - T_c$. This equation holds for homogeneous nucleation from a melt near the melting temperature. To apply this to a heterogeneous nucleating agent, Eq. 12 is transformed to the following:

$$\ln \phi = A - (B^*/\Delta T_c^2) \tag{13}$$

Figure 7 presents the relationship between of $\ln \phi$ and $1/\Delta T_c^2$ for the neat PP and composite samples. As can be seen, a series of straight lines are obtained in both samples ($R^2 > 0.998$). From the slope, the values of B and B^* are 6.1×10^3 and $5.1 \times 10^3 \text{ K}^2$, respectively. Then by computing from Eq. 10, the nucleation activity (ϕ) of the 10 wt%TLCP/PP sample was 0.83. This indicates the incorporation of in situ formed TLCP fibrils acting effectively as a heterogeneous nucleation agent in the PP matrix.

Thermal stability of 10 wt%TLCP/PP composite film

Thermogravimetric (TG) and corresponding differential thermogravimetric (DTG) thermograms of the neat PP and

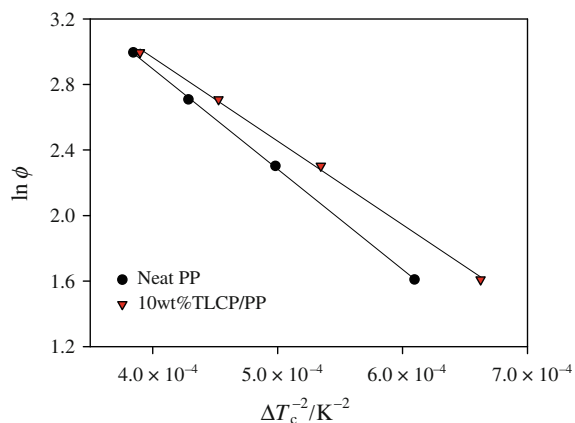


Fig. 7 Relationship between $\ln \phi$ and $1/\Delta T_c^2$ for calculating the nucleation activity of neat PP and 10 wt% TLCP/PP films

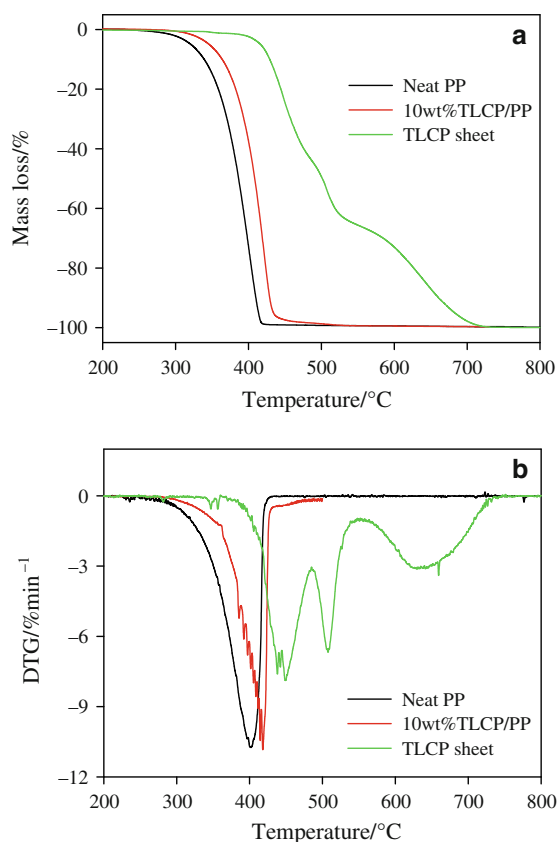


Fig. 8 **a** TG and **b** DTG thermograms of neat PP film, 10 wt% TLCP/PP film and TLCP sheet measured at a scanning rate of $10\text{ }^\circ\text{C min}^{-1}$ under N_2 atmosphere

10 wt% TLCP/PP films measured at a heating rate of $10\text{ }^\circ\text{C min}^{-1}$ in N_2 are presented in Figs. 8a and b, respectively. Clearly, the neat PP film occurred in only single-step mass loss at temperature of 300–450 $^\circ\text{C}$ (see Fig. 8a) with one maximum rate peak at 402 $^\circ\text{C}$ (see Fig. 8b), corresponding to the decomposition of PP backbone comprising

Table 3 Parameters evaluated from TG and DTG thermograms of neat PP film, 10 wt% TLCP/PP film and TLCP sheets

Samples	$T_i/^\circ\text{C}$	$T_{\max}/^\circ\text{C}$	$\Delta E/\text{kJ mol}^{-1}$
Neat PP	362	402	159
10 wt% TLCP/PP	373	418	183
TLCP sheet ^a	417	450	221

^a Evaluated from the first thermal decomposition stage only

of the two pathways of mechanism which occurred simultaneously [38]. On the contrary, the TLCP (Rodrun LC5000) sheet exhibited three-step decompositions at temperature of 410–730 $^\circ\text{C}$ (see Fig. 8a) with three maxima rate peaks at 450, 510, and 630 $^\circ\text{C}$ (see Fig. 8b), respectively. The first two-steps decomposition corresponds to the decomposition of PET component and the final step corresponds to the decomposition of HBA component. For the 10 wt% TLCP/PP films, a single-step weight loss was observed with its corresponding maximum rate peak at 418 $^\circ\text{C}$. The onset (T_{onset}) and maximum (T_{max}) decomposition temperatures of the samples are summarized in Table 3. It is seen that both T_{onset} and T_{max} of the composite film are higher than those of the neat PP film, indicating that incorporation of TLCP phase leads to the improvement of thermal stability of PP matrix. These data agree well with the TG results of extruded stands of TLCP/PP blends reported by Saikrasun and Saengsuwan [39].

The activation energy (ΔE) for thermal degradation of the samples was evaluated from the TG curves using the method of Horowitz and Metzger [40] as follows:

$$\ln[\ln(W_0/W_T)] = \Delta E\theta/RT_{\max}^2 \quad (14)$$

where W_0 and W_T are the initial and residual weight of the polymer at temperature T , and θ is $T - T_{\max}$. The activation energies were obtained from the slope of the plot of $\ln[\ln(W_0/W_T)]$ versus θ (see Table 3), as presented in Fig. 9.

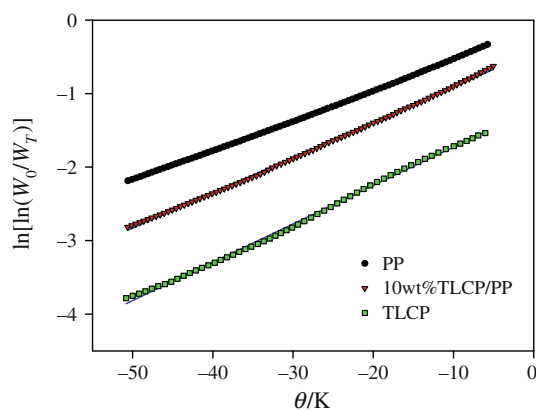


Fig. 9 Plot of $\ln[\ln(W_0/W_T)]$ versus θ for calculating the decomposition activation energy of the neat PP film, 10 wt% TLCP/PP film and TLCP sheet

The decomposition activation energies of neat PP, 10 wt% TLCP/PP and TLCP are 159, 183 and 221 kJ mol⁻¹, respectively. The ΔE of composite sample is remarkable higher than that of neat PP film, corresponding to their T_{onset} and T_{max} . This result suggests that TLCP fibrils in situ formed in PP matrix during processing can significantly improve the thermal stability of PP blend.

Conclusions

The study on non-isothermal crystallization kinetics and thermal stability of the composite influenced by in situ formed TLCP fibrils using DSC and TGA, respectively, showed that the T_c and $t_{1/2}$ of composite films were higher and lower than those of neat PP films at each cooling rate, respectively. This suggested that the overall crystallization rate of composite film was faster than that of neat PP one. Also, it was implied that TLCP fibrils acted as heterogeneous nucleating sites in PP matrix. To analyze the non-isothermal crystallization kinetics of samples, three kinetic models; modified Avrami, Ozawa, and Mo methods, were employed. The studies demonstrated that Mo method successfully described the non-isothermal crystallization process in both systems. The $F(T)$ values of the composite film were smaller than that of neat PP film, suggesting the faster crystallization rate of PP in the composite due to the nucleating effect of in situ generated TLCP fibers in PP phases. The crystallization activation energy based on Kissinger method of the composite was found to be much smaller than that of PP film, indicating the easier movement of PP molecular chains in the TLCP/PP systems which subsequently resulted in the faster crystallization rate of PP. In addition, the calculated nucleation activity of composite agreed very well with the reduction of $t_{1/2}$, $F(T)$ and crystallization activation energy in the composite sample.

Finally, the thermal stability of the composite film was also investigated in N₂ atmosphere. The results revealed that both T_{onset} and T_{max} of the composite were shifted to higher temperatures. Also, the decomposition activation energy of the composite was higher than that of PP. These results suggested that in situ forming of TLCP fibrils in PP matrix significantly improved the thermal stability of composite which could extend the application ranges of TLCP/PP composites.

Acknowledgements This study was funded by a grant from the Thailand Research Fund (MRG4780032). Partial financial supports from the Center for Innovation in Chemistry (PERCH-CIC), Commission on Higher Education, Ministry of Education and Ubon Ratchathani University are also acknowledged. The SS author also grateful thanks to Prof. Saivarop Bualek-Limcharoen for providing TLCP and giving the useful discussion.

References

1. Handlos AA, Baird DGB. Processing and associated of in situ composites based on thermotropic liquid crystalline polymers and thermoplastics. *JMS Rev Macromol Chem Phys.* 1995;C35(2): 183–238.
2. Jin X, Li W. Correlation of mechanical properties with morphology, rheology, and processing parameters for TLCP containing blends. *JMS Rev Macromol Chem Phys.* 1995;35(1): 1–13.
3. Tjong SC. Structure, morphology, mechanical and thermal characteristics of the in situ composites based on liquid crystalline polymers and thermoplastics. *Mater Sci Eng Rep.* 2003;41: 1–60.
4. Dutta D, Fruitwala H, Kohli A, Wiess RA. Polymer blends containing liquid crystals and thermoplastics. *Polym Eng Sci.* 1990;30:1005–18.
5. Qin Y, Brydon DL, Mather RR, Wardman RH. Fibers from polypropylene and liquid crystalline blends: 3. A comparison of polyblend fibers containing Vectra A900, Vectra B950 and Rodrun LC3000. *Polymer.* 1993;34:3597–604.
6. Saengsuwan S, Bualek-Limcharoen S, Mitchell GR, Olley RH. Thermotropic liquid crystalline polymer (Rodrun LC5000)/polypropylene in situ composite films: rheology, molecular orientation and tensile properties. *Polymer.* 2003;44:3407–15.
7. Kiss G. In situ composites: blends of isotropic polymers and thermotropic liquid crystalline polymers. *Polym Eng Sci.* 1987;27(6):410–23.
8. Blizard KG, Baird DG. The morphology and rheology of polymer blends containing a liquid crystalline copolyester. *Polym Eng Sci.* 1987;27:653–62.
9. Wu S. Formation of dispersed phase in incompatible polymer blends: Interfacial and rheological effects. *Polym Eng Sci.* 1987;27(5):335–43.
10. Heino MT, Vainio TP. In: Cheremisinoff NP, Cheremisinoff PN, editors. Effect of viscosity ratio and processing conditions on the morphology of blends of liquid crystalline polymer and polypropylene. *Handbook of applied polymer processing technology.* New York: Marcel Dekker, Inc.; 1996.
11. Xu QW, Man HC, Lau WS. The effect of a third component on the morphology and mechanical properties of liquid-crystalline polymer and polypropylene in situ composites. *Comp Sci Technol.* 1999;59:291–6.
12. Xu W, Ge M, He P. Non-isothermal crystallization kinetics of polypropylene/montmorillonite nanocomposites. *J Appl Polym Sci B.* 2002;40:408–14.
13. Papageorgiou GZ, Achilias DS, Bikiaris DN, Karayannidis GP. Crystallization kinetics and nucleation activity of filler in polypropylene/surface-treated SiO₂ nanocomposites. *Thermo Acta.* 2005;427:117–28.
14. Jain S, Goossens H, Dulin MV, Lemstra P. Effect of in situ prepared silica nano-particles on non-isothermal crystallization of polypropylene. *Polymer.* 2005;46:8805–18.
15. Varga J. In: Karger-Kocsis J, editor. Polypropylene: structure, blends and composites, vol 1, chap 3. London: Chapman and Hall; 1995.
16. Friedrich K, Evstatiev M, Fakirov S, Evstatiev O, Ishii M, Harrass M. Microfibrillar reinforced composites from PET/PP blends: Processing, morphology and mechanical properties. *Comp Sci Technol.* 2005;65(1):107–16.
17. Zhang H, Zhang Q, Sun C. Nonisothermal crystallization kinetics of polypropylene/polyethersulfone blend. *Polym Bull.* 2008;60: 291–300.
18. Sukananta P, Bualek-Limcharoen S. In situ modulus enhancement of polypropylene monofilament through blending with

- liquid-crystalline copolyester. *J Appl Polym Sci.* 2003;90:1337–46.
19. Minkova LI, Paci M, Pracella M, Magagnini P. Crystallization behavior of polyphenylene sulfide in blends with a liquid crystalline polymer. *Polym Eng Sci.* 1992;32:57–64.
 20. Yan H, Xu J, Mai K, Zeng H. Crystallization of poly(butylene terephthalate) blends containing liquid crystalline polymer component. *Polymer.* 1999;40:4865–75.
 21. Gopakumar TG, Ghadage RS, Ponrathnam S, Rajan CR, Fradet A. Poly(phenylene sulfide)/liquid crystalline polymer blends: 1. Non-isothermal crystallization kinetics. *Polymer.* 1997;38(9):2209–14.
 22. Minkova L, Magagnini PL. Blends of poly(ethylene 2,6-naphthalate) with liquid-crystalline polymers: crystallization behavior and morphology. *Polymer.* 2001;42(13):5607–13.
 23. Pracella M, Dainelli D, Galli G, Chiellini E. Polymer blends based on mesomorphic components, 1. Properties of poly(tetramethylene terephthalate)/poly(decamethylene 4,4-terephthaloyldixybenzoate) blends. *Makromol Chem.* 1986;187:2387–400.
 24. Carvalho B, Bretas ERS. Crystallization kinetics of a PEEK/LCP blend. *J Appl Polym Sci.* 1994;55(2):233–46.
 25. Torre FJ, Cortazar MM, Gomez MA, Ellis G, Marco C. Isothermal crystallization of iPP/Vectra blends by DSC and simultaneous SAXS and WAXS measurements employing synchrotron radiation. *Polymer.* 2003;44:5209–17.
 26. Tjong SC, Chen SX, Li RKY. Crystallization kinetics of compatibilized blends of a liquid crystalline polymer with polypropylene. *J Appl Polym Sci.* 1997;64:707–15.
 27. Durmus A, Yalçımyuva T. Effects of additives on non-isothermal crystallization kinetics and morphology of isotactic polypropylene. *J Polym Res.* 2009;16:489–98.
 28. Avrami M. Kinetics of phase change II. Transformation-time relations for random distribution of nuclei. *J Chem Phys.* 1940;8(2):212–24.
 29. Jeziorny A. Parameters characterizing the kinetics of the non-isothermal crystallization of poly(ethylene terephthalate) determined by DSC. *Polymer.* 1978;19(10):1142–4.
 30. Mandelkern L. Crystallization of polymers: kinetics and mechanisms. 2nd ed. Cambridge: Cambridge University Press; 2004.
 31. Ozawa T. Kinetics of non-isothermal crystallization. *Polymer.* 1971;12(3):150–8.
 32. Kalkar AK, Deshpande VD, Kukarni MJ. Nonisothermal crystallization kinetics of poly(phenylene sulphide) in composites with a liquid crystalline polymer. *J Polym Sci B.* 2010;48:1070–100.
 33. Long Y, Shanks RA, Stachurski ZH. Kinetics of polymer crystallization. *Prog Polym Sci.* 1995;20:651–701.
 34. Liu T, Mo Z, Wang S, Zhang H. Nonisothermal melt and cold crystallization kinetics of poly(aryl ether ether ketone ketone). *Polym Eng Sci.* 1997;37(3):568–75.
 35. Kissinger HE. Variation of peak temperature with heating rate in differential thermal analysis. *J Res Natl Bur Stand.* 1956;57:217–21.
 36. Dobrev A, Gutzow I. Activity of substrates in the catalyzed nucleation of glass-forming melts. II. Experimental evidence. *J Non-Cryst Solids.* 1993;162:13–25.
 37. Dobrev A, Gutzow I. Activity of substrates in the catalyzed nucleation of glass-forming melts. I. Theory. *J Non-Cryst Solids.* 1993;162:1–12.
 38. Peterson JD, Vyazovkin S, Wight CA. Kinetics of thermal and thermo-oxidative degradation of polystyrene, ethylene and poly(propylene). *Macromol Chem Phys.* 2001;202:775–84.
 39. Saikrasun S, Saengsuwan S. Thermal decomposition kinetics of in situ reinforcing composite based on polypropylene and liquid crystalline polymer. *J Mater Process Technol.* 2009;209:3490–500.
 40. Horowitz HH, Metzger G. A new analysis of thermogravimetric traces. *Anal Chem.* 1963;35:1464–71.